Bursts of small icebergs: drifting and melting breakwaters in the Southern Ocean

Jean Tournadre, Fabrice Ardhuin, Pierre Queffeulou, and Fanny Girard-Ardhuin

Ifremer, Laboratoire d'Océanographie Spatiale, Plouzané, France

The variability of small-size iceberg distributions is revealed from a novel analysis of satellite altimeter data. A strong annual cycle is modulated by pulse-like events confined to single ocean basins, with dense iceberg populations in the South Atlantic in 2003-2005, and in the South Pacific in 2008. Anomalies in sea surface temperatures of the order of 1°C may be related to the iceberg distribution. Icebergs also appear very strongly associated with anomalies in the heights of ocean waves. A preliminary parameterization of wave blocking by icebergs significantly reduces wave model errors in the region south of 45° South, and has a perceptible influence on all the west coasts of the Southern hemisphere.

1. Introduction

The distribution of icebergs less than 6 km in length, has been known from ship-based observations [e.g. *Jacka and Giles*, 2006] a synthetic aperture radar analyses [*Williams et al.*, 1999] with a limited temporal and spatial coverage. These small icebergs may account for a significant part of the freshwater volume flux delivered by icebergs to the Southern Ocean [*Silva et al.*, 2006], with an associated iron flux important for the ocean primary productivity [*Smith et al.*, 2007]. Recently, *Tournadre et al.* [2008] demonstrated that small icebergs, with areas in the range 0.5 to 30 km^2, have a significant signature in the noise part of high resolution altimeter waveforms, that can be analyzed to determine their distribution. Here we present the first climatology of small icebergs for the entire Southern ocean, and analyze its relationship with other observations, in particular wave heights.

0094-8276/10/$5.00

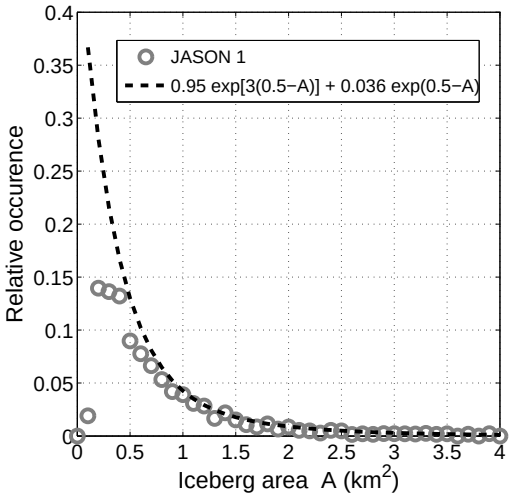

Figure 1. Normalized distribution of iceberg areas detected using Jason-1 altimeter data, for the year 2004. The dashed line shows a fit of the histogram used for numerical wave modeling.

2. Analysis

Besides the detection of icebergs, the analysis of altimeter waveforms also provides the icebergs elevation h, while the iceberg area A is related to the radar backscatter strength. The Jason-1 altimeter archive, from 2002 to 2008, has been processed to produce a database of small icebergs over the southern Ocean (south of 45° S).

Although the coverage of the ocean by a single satellite is limited to a narrow swath, about 6-8 km wide, the sampling rate is high enough to yield a reliable estimate of the probability P of presence of an iceberg, at time and space resolutions of 1 month and 100 km respectively. That resolution is close to the Jason-1 track spacing at 50° latitude, which has a 10 day repeat cycle. The number of Jason passes increased markedly towards the high latitudes, providing more robust iceberg statistics. We estimate ice volumes from iceberg areas, assuming that 90% of the volume is underwater,

$$V(i,j,t) = 10P(i,j,t)A(i,j,t)h(i,j,t)\frac{\Delta x \Delta y}{A_{SW}} \qquad (1)$$

with $A(i,j,t)$ the average iceberg area, $(\Delta x, \Delta y)$ the sampling grid spacing and A_{SW} the area of the altimeter field of view. The histogram of iceberg sizes for the entire Southern ocean and all the year 2004 is shown in figure 1. The altimeter is not expected to properly detect all icebergs with areas less than 0.5 km^2. Although the missed small icebergs contribute little to the ice volume, they may have a significant effect on the propagation of ocean waves.

3. Results

Integrating the iceberg volume in the open ocean (outside of sea ice) from 65°S to 45°S, the outstanding pattern revealed by Figure 2.a is the predominance of the South Atlantic sector (50°W to 30°E) with most small icebergs formed in the Weddell sea during the austral summer. In that sector, the ice volume can exceed 100 Gt (Figure 2.d), and a significant amount of ice reaches as far as 45°S in late 2003 (Figure 3.a). The year to year variation of the ice volume is important, with bursts of iceberg formation occurring in 2003-2004 in the South Atlantic, and in 2008 in the Ross sea. A strong negative anomaly in sea water temperature is found around large concentrations of icebergs, in the South Pacific in 2008, and South Atlantic in 2003-2004 (Figure 2.b). Although not systematic, these patterns can be caused by iceberg melting, which, previously, could only be inferred from runoff estimates for Antarctica and a modeling of iceberg drift [e.g. *Gladstone et al.*, 2001].

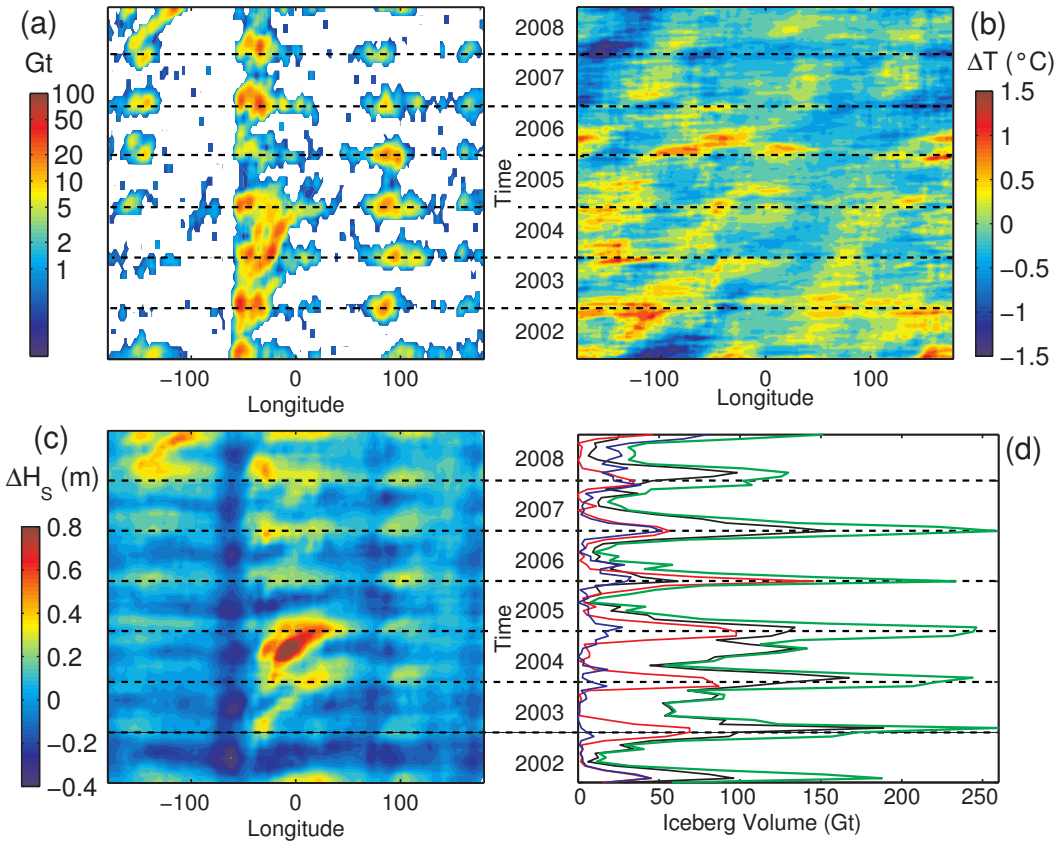

Figure 2. Longitude-time Hovmöller diagrams of (a) the total volume of small icebergs between latitudes 65°S and 45°S, over a 2° sector in longitude, (b) sea surface temperature anomaly estimated using the weekly NOAA Optimum Interpolation Sea Surface Temperature Version2 [*Reynolds et al.*, 2002]). (c) Biases of modeled significant wave heights [*Ardhuin et al.*, 2010] relative to satellite altimeter measurements [*Queffeulou and Croizé-Fillon*, 2010]. (d) Total volume of small icebergs from the whole southern ocean (green), and the south Atlantic ocean (50°W to 30°E, black), south Indian ocean (50°E to 130°E red) and South Pacific ocean (130°E to 100° W, red).

The errors of a numerical wave model that does not account for icebergs, provides an independent verification of our iceberg detection. This wave model is based on the WAVEWATCH III^{TM} code [*Tolman*, 2008] and forced by analyzed winds and sea ice mask from ECMWF, treated with the subgrid method by *Tolman* [2003]. Both forcing and model have a resolution of 0.5° in longitude and latitude. The model without iceberg effects is described by *Magne et al.* [2010], using the TEST441 parameterization proposed by *Ardhuin et al.* [2009]. This model generally provides very accurate estimate of sea states without any assimilation of wave data [*Bidlot*, 2008]. Model results for the significant wave height H_s are compared with observations derived from all available satellite altimeters, as calibrated by *Queffeulou and Croizé-Fillon* [2010]. The comparison method is taken from *Rascle et al.* [2008].

Model biases are less than 30 cm except for latitudes 65°S to 45°S, where the positive bias pattern is very similar to iceberg concentrations, with the same strong space-time variability. The bias pattern, is shifted by 5 to 10° to the East of the iceberg distribution. (Figure 2.c). This shift is consistent with the expected partial blocking of the wave energy flux, predominantly oriented eastward. Namely, the model that does not account for icebergs is overestimating the wave heights in the regions that are, in reality, sheltered by the icebergs. The general negative bias in 2002 is related to stronger negative biases in modeled winds before 2003. Given the impact of waves on nearshore and upper ocean mixing, large gradients in wave height at the scale of individual icebergs probably enhance the mixing of water properties, while the icebergs also induce wind-driven upwelling.

Beyond these local effects of icebergs on the sea state, the errors in modeled significant wave height also appear to propagate further North, beyond the regions covered with icebergs (figures 3.d,e,f).

4. Wave modeling with icebergs

In order to understand this remote effect, we defined a first simple parameterization of the icebergs as moving subgrid obstacles, following the treatment of (fixed) subgrid islands and (moving) marginal ice by *Tolman* [2003]. Assuming square icebergs that completely absorb the wave energy flux that they intercept, the proportion r of the incoming wave energy flux blocked by icebergs over a unit propagation distance (here 1 km) is the length of the icebergs, in the direction perpendicular to the propagation, per unit propagation distance. For an individual rectangular iceberg perpendicular to the wave propagation direction, the iceberg area is this length multiplied by a width.

For a not too dense population of icebergs, we may neglect the probability that two icebergs may be aligned in the wave propagation direction, and r is given by the ratio

$$r(i,j,t) = C(i,j,t)/W(i,j,t) \qquad (2)$$

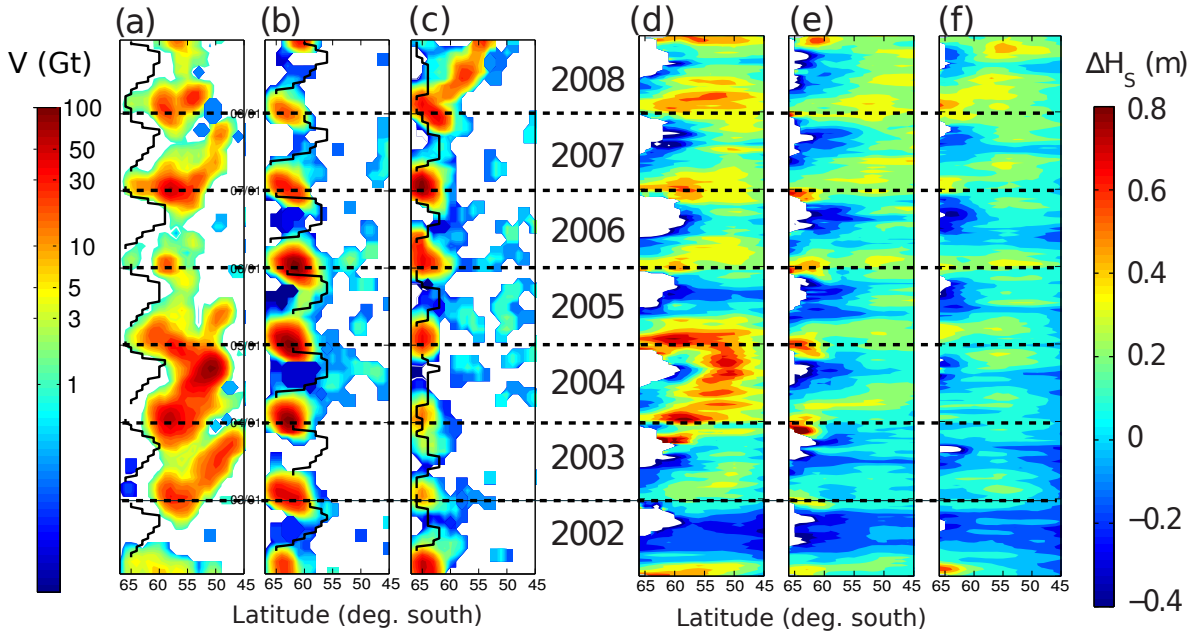

Figure 3. Latitude-time Hovmöller diagrams of the small iceberg ice volume over each 2° band of latitude for (a) the South Atlantic 50°W to 30°E, (b) the Indian Ocean 50°E to 130° E, (c) the South Pacific 130°E to 100° W. (d), (e), and (f) significant wave height model bias against satellite altimeters for the same three sectors of the Southern Ocean, for a model without iceberg effects. In the left panels (a,b,c) the black line marks the annual maximum extent of the sea ice, and in the right panels (d,e,f) the white areas give the minimum extent of the 80% sea ice coverage, used as a mask in the model.

of the fraction of sea area covered by icebergs,

$$C(i,j,t) = P(i,j,t)\frac{A(i,j,t)}{A_{SW}} \tag{3}$$

and an effective iceberg width in the wave propagation direction

$$W = \sum_k C_0(k)A_0(k) / \sum_k C_0(k)\sqrt{A_0(k)} \tag{4}$$

where k is the iceberg size index, and $C_0(k)$ is the number of icebergs of area $A_0(k)$. Here C_0 was taken uniform in space and time, i.e. independent of i, j and t. As a result W is a constant that only depends on the iceberg size histogram. r is a spatial decay rate, with units of km^{-1}. The fitted size distribution shown in figure 1 gives $W = 0.85$ km. Here $C(i,j,t)$ reaches as much as 1.2%, corresponding to a decay $r = 0.02$ km^{-1}, or an e-folding scale $1/r$ of 50 km. This scale is very short compared to the growth scale of waves in strong winds which is of the order of 300 to 1000 km [*Sverdrup and Munk*, 1947]. More typical values $r \simeq 0.002$ km^{-1} give attenuation scales comparable to the wind-wave growth scales.

If the histogram were restricted to icebergs larger than 0.5 km^2, we would get an effective iceberg width $W = 1.6$ km (in the direction of wave propagation), and, according to eq. (2), a weaker effect on waves. This illustrates the importance of the smallest icebergs, which should still have lengths larger than the dominant wavelength of wind-waves, i.e. a few hundred meters, to have any strong blocking effect.

Here we show model results obtained with W set to 0.42 km. This reduction of W, which increases the local iceberg effect by a factor of two, was first motivated by the fact that it gave a slightly better result in terms of wave heights. Why the model fits the data better for $W < 0.8$ km is likely the result of the geometry of the icebergs that are not square. From the analysis of a few synthetic aperture radar images [see also *Williams et al.*, 1999], small icebergs appear to have their longer side perpendicular to the wave direction, which is why we termed length the dimension is that direction. A smaller W can also be the result of a varying size histogram with, in reality, a larger proportion of small icebergs away from the Antarctic continent.

The wave model is validated with measurements of wave height from all altimeters (in the case of figure 4, these are Jason-1, ENVISAT and GFO), which, given the low probability of iceberg detection, are practically independent from the Jason-derived iceberg data. The variability of wave heights is much better captured in the model that includes parametrized icebergs (Figure 4) with a reduction of the normalized root mean square error (NRMSE) by 12% for the region South of 45°S during the year 2008. This includes a significant improvement (10% reduction in error) of the model results along all the South-American continent due to a better representation of swells propagated from the Southern ocean.

The model suggests that for a single wave event, icebergs at 60° South may reduce wave heights by 20 cm as far as 10° South (figure 4.c). This improved variability of the model, with a very limited change in the mean wave heights (2% reduction over the ocean south of 45° S) provides a solid verification of the reality of the iceberg population patterns derived from the altimeter data. Similar results are found for other years, with stronger impacts in 2004. All these model results and the iceberg masks are available from http://tinyurl.com/yetsofy.

The global iceberg database presented here reveal an annual cycle with a large interannual variability. Because the strong bursts of small icebergs are likely related to the Antarctic meteorology, which also defines wind patterns and ocean convection worldwide [*Swingedouw et al.*, 2009], they are probably not the initial cause of interannual variability of other Southern Ocean properties. However, these

icebergs are related to large anomalies in sea surface temperatures and they also strongly impact ocean waves, with a far-reaching impact that was illustrated here with their mechanical blocking influence on swells in the Pacific, that affects the South American coasts. Although we found no clear relashionship between iceberg bursts and ocean color anomalies, as expected from [e.g. *Smith et al.*, 2007], the present findings call for a continued monitoring of icebergs and their associated freshwater and nutrient flux to the Southern Ocean. For this, altimeter data is complementary to synthetic aperture radar data that is best used for calibration on limited areas, due to the large volume of acquisitions and processing required.

Acknowledgments. F.A. is funded by ERC grant #240009 "IOWAGA" and U.S. National Ocean Partnership Program, under grant N00014-10-1-0383. Altimeter data from Jason-1 was kindly provided by CNES through AVISO. The suggestions of anonymous reviewers were very helpful.

References

Ardhuin, F., L. Marié, N. Rascle, P. Forget, and A. Roland (2009), Observation and estimation of Lagrangian, Stokes and Eulerian currents induced by wind and waves at the sea surface, *J. Phys. Oceanogr.*, *39*(11), 2820–2838.

Ardhuin, F., et al. (2010), Semi-empirical dissipation source functions for wind-wave models: part I, definition, calibration and validation, *J. Phys. Oceanogr.*, *40*(9), 1917–1941.

Bidlot, J.-R. (2008), Intercomparison of operational wave forecasting systems against buoys: data from ECMWF, MetOffice, FNMOC, NCEP, DWD, BoM, SHOM and JMA, September 2008 to November 2008, *Tech. rep.*, Joint WMO-IOC Technical Commission for Oceanography and Marine Meteorology, available from http://preview.tinyurl.com/7bz6jj.

Gladstone, R. M., G. R. Bigg, and K. W. Nicholls (2001), Iceberg trajectory modeling and meltwater injection in the Southern Ocean, *J. Geophys. Res.*, *106*(C9), 19,903–19,915.

Jacka, T. H., and A. B. Giles (2006), Antarctic iceberg distribution and dissolution from ship-based observations, *J. Glaciol.*, *53*, 341–356.

Magne, R., F. Ardhuin, and A. Rolan (2010), Prévisions et rejeux des états de mer du globe à la plage (waves forecast and hincast from global ocean to the beach), *European Journal of Environmental and Civil Engineering*, *14*, 149–162, doi: 10.3166/ejece.14.149-162.

Queffeulou, P., and D. Croizé-Fillon (2010), Global altimeter SWH data set, version 7, may 2010, *Tech. rep.*, Ifremer, uRL:http://tinyurl.com/2cj5sez.

Rascle, N., F. Ardhuin, P. Queffeulou, and D. Croizé-Fillon (2008), A global wave parameter database for geophysical applications. part 1: wave-current-turbulence interaction parameters for the open ocean based on traditional parameterizations, *Ocean Modelling*, *25*, 154–171, doi:10.1016/j.ocemod.2008.07.006.

Reynolds, R. W., N. Rayner, T. Smith, D. Stokes, and W. Wang (2002), An improved in situ and satellite SST analysis for climate, *J. Climate*, *15*, 1609–1625.

Silva, T. A. M., G. R. Bigg, and K. W. Nicholls (2006), Contribution of giant icebergs to the southern ocean freshwater flux, *J. Geophys. Res.*, *111*, C03,004, doi:10.1029/2004JC002843.

Smith, K. L., Jr., B. H. Robison, J. J. Helly, R. S. Kaufmann, H. A. Ruhl, T. J. Shaw, B. S. Twining, and M. Vernet (2007), Free-drifting icebergs: Hot spots of chemical and biological enrichment in the Weddell sea, *Science*, *317*, 478–482.

Sverdrup, H. U., and W. H. Munk (1947), Wind, sea, and swell: theory of relations for forecasting, *Tech. Rep. 601*, U. S. Hydrographic Office.

Swingedouw, D., T. Fichefet, H. Goosse, and M. F. Loutre (2009), Impact of transient freshwater releases in the southern ocean on the amoc and climate, *Climate Dynamics*, *33*, 365–381.

Tolman, H. L. (2003), Treatment of unresolved islands and ice in wind wave models, *Ocean Modelling*, *5*, 219–231.

Tolman, H. L. (2008), A mosaic approach to wind wave modeling, *Ocean Modelling*, *25*, 35–47, doi: 10.1016/j.ocemod.2008.06.005.

Tournadre, J., K. Whitmer, and F. Girard-Ardhuin (2008), Iceberg detection in open water by altimeter waveform analysis, *J. Geophys. Res.*, *113*(7), C08,040, doi:10.1029/2007JC004587.

Williams, R. N., W. G. Rees, and N. W. Young (1999), A technique for the identification and analysis of icebergs in synthetic aperture radar images of Antarctica, *Int. J. Remote Sensing*, *20*(15), 3183–3199.

Fabrice Ardhuin, Ifremer, Laboratoire d'Océanographie Spatiale, BP70, 29280 Plouzané, France. (ardhuin@ifremer.fr)

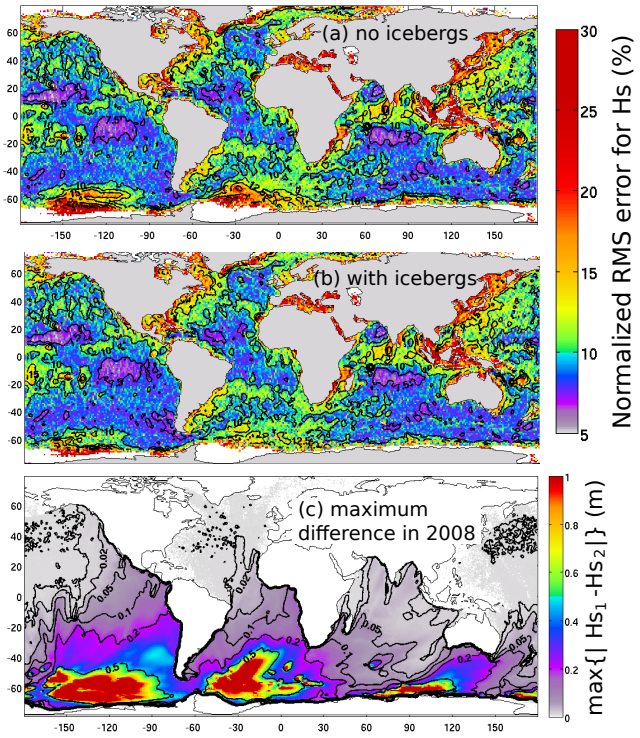

Figure 4. Impact of iceberg in model errors for the significant wave height H_s. The top panel shows the model normalized root mean square error against altimeter measurements of H_s, for the year 2008. This is similar to figure 11 in *Ardhuin et al.* [2010]. The middle panel show the same error measure for a model that includes a representation of icebergs. Contours are drawn for 7.5, 10, 12.5, 15 and 20% error levels. The bottom panel show the maximum difference, in meters, over the year 2008, between modeled wave heights without (Hs_1) and with (Hs_2) icebergs.